© 2002 The Chemical Society of Japan Bull. Chem. Soc. Jpn., 75, 2595–2607 (2002)

Alkoxo-Bridged Dinuclear and Tetranuclear Copper(II) Complexes with Schiff-Bases Derived from Benzoylacetone and 1,*n*-Diamino-*n*′-hydroxyalkanes (*n*, *n*′ = 3, 2; 4, 2; and 5, 3)

Masahiro Mikuriya,* Kenichi Minowa, and Ryoji Nukada

Department of Chemistry, School of Science and Technology, Kwansei Gakuin University, Gakuen 2-1, Sanda 669-1337

(Received April 8, 2002)

Alkoxo-bridged copper(II) complexes with *N*,*N*′-bis(1-methyl-3-hydroxy-3-phenyl-2-propen-1-ylidene)-1,3-diamino-2-propanol (H_3bzacpro), *N*,*N*′-bis(1-methyl-3-hydroxy-3-phenyl-2-propen-1-ylidene)-1,4-diamino-2-butanol (H_3bzacbu), and *N*,*N*′-bis(1-methyl-3-hydroxy-3-phenyl-2-propen-1-ylidene)-1,5-diamino-3-pentanol (H_3bzacpen), [Cu_2(bzacpro)(CH_3CO_2)] (**1**), [Cu_4(bzacpro)$_2$(C_2H_5O)$_2$] (**2**), [Cu_2(bzacbu)(CH_3CO_2)] (**3**), [Cu_4(bzacbu)$_2$(CH_3O)$_2$] (**4**), [Cu_4(bzacpen)$_2$(CH_3CO_2)$_2$] (**5**), and [Cu_4(bzacpen)$_2$O]·H_2O (**6**) have been synthesized and characterized by measurements of the infrared and electronic spectra, and the magnetic susceptibilities. Single-crystal X-ray analyses revealed that **1** and **3** are dinuclear copper(II) complexes having a dinuclear core bridged by an alkoxo-oxygen atom of bzacpro or bzacbu and acetato-oxygen atoms, whereas **2**, **4**, **5**, and **6** are tetranuclear copper(II) complexes composed of μ-alkoxo(bzacpro)-μ-ethoxo-, μ-alkoxo(bzacbu)-μ-methoxo-, μ-alkoxo(bzacpen)-μ-acetato-, and μ-alkoxo(bzacpen)-μ-oxo-bridged units, respectively. Magnetic-susceptibility data show that an antiferromagnetic interaction is operative within the dinuclear or tetranuclear core in **1**–**3**, **5** and **6**, whereas a ferromagnetic coupling is operative in **4**. The crystal structures of the three Schiff-base ligands have also been elucidated.

There has been much interest in the past years in alkoxo-bridged copper(II) complexes, with particular interest directed towards the magnetostructural correlation between the magnetic properties and the crystal structures, especially the relationship between the magnetic coupling constant (2*J*) and the Cu–O–Cu angle.[1–12] The alkoxo-bridged dinuclear copper(II) complexes have also been studied in the context of modeling biological systems, because dinuclear copper centers have important functional roles in the active sites of copper-containing proteins, such as hemocyanin, tyrosinase, and catecol oxidase.[13–20] An example of such a model is an alkoxo-bridged dinuclear complex with *N*,*N*,*N*′,*N*′-tetrakis[2-(1-ethylbenzimidazolyl)methyl]-1,3-diamino-2-propanol, reported by Reed et al.[16] They utilized a dinucleating ligand having 1,3-diamino-2-propanolate as a bridging skelton. This kind of polydentate ligand which has an alcoholic group is useful to design the synthesis of endogenous-alkoxo-bridged dinuclear metal complexes.[16–36] Among these dinucleating ligands, *N*,*N*′-bis(1-methyl-3-hydroxy-3-phenyl-2-propen-1-ylidene)-1,3-propanediamino-2-propanol (abbreviated as H_3bzacpro, Scheme 1) is unique, because the Schiff-base ligand possesses a dinucleating functionality that can serve as a bridging alkoxo group in addition to keto-oxygen and imino-nitrogen atoms, and also give oligonuclear metal species with interesting physicochemical properties. So far, a variety of oligonuclear structures have been elucidated for complexes of manganese, iron, cobalt, nickel, and zinc ions by the X-ray crystallography.[36] However, no oligonuclear structures have been found in a copper system, although some alkoxo-bridged dinuclear copper(II) structures were reported.[32] We have therefore made a detailed and further study to extend this copper system by using analogous Schiff-base ligands additionally. Herein we report on the synthesis, crystal structures, and magnetic properties of alkoxo-bridged copper(II) complexes with *N*,*N*′-bis(1-methyl-3-hydroxy-3-phenyl-2-propen-1-ylidene)-1,3-diamino-2-propanol (H_3bzacpro), *N*,*N*′-bis(1-methyl-3-hydroxy-3-phenyl-2-propen-1-ylidene)-1,4-diamino-2-butanol (H_3bzacbu), and *N*,*N*′-bis(1-methyl-3-hydroxy-3-phenyl-2-propen-1-ylidene)-1,5-diamino-3-pentanol (H_3bzacpen) as well as the crystal structures of the free Schiff-base ligands (Scheme 1).

Experimental

Synthesis of the Schiff-Base Ligands. 1,3-Diamino-2-propanol was obtained from Tokyo Kasei Kogyo Co., Ltd. 1,4-Diamino-2-butanol and 1,5-diamino-3-pentanol were synthesized according to a method reported elsewhere.[28]

***N*,*N*′-Bis(1-methyl-3-hydroxy-3-phenyl-2-propen-1-ylidene)-1,3-diamino-2-propanol (H_3bzacpro).** 1,3-Diamino-2-propanol (1.80 g, 20.0 mmol) was dissolved in methanol (25 cm^3) and added to a solution of benzoylacetone (6.49 g, 40.0 mmol) in methanol (25 cm^3). The mixed solution was refluxed for 0.5 h and then allowed to stand overnight at 5 °C. The resulting white crystals were filtered, washed with diethyl ether and dried in vacuo over P_2O_5. Yield, 5.47 g (72.0%). Found: C, 72.68; H, 6.89; N, 7.57%. Calcd for $C_{23}H_{26}N_2O_3$: C, 72.99; H, 6.92; N, 7.40%. IR (KBr) ν(C=O) 1598 (s), ν(C=C) 1578 (s), 1535 (s), 1437, 1317, 1289 cm^{-1}.

***N*,*N*′-Bis(1-methyl-3-hydroxy-3-phenyl-2-propen-1-ylidene)-1,4-diamino-2-butanol (H_3bzacbu).** 1,4-Diamino-2-butanol (0.52 g, 5.0 mmol) was dissolved in methanol (7 cm^3) and added to a solution of benzoylacetone (1.62 g, 10.0 mmol) in methanol

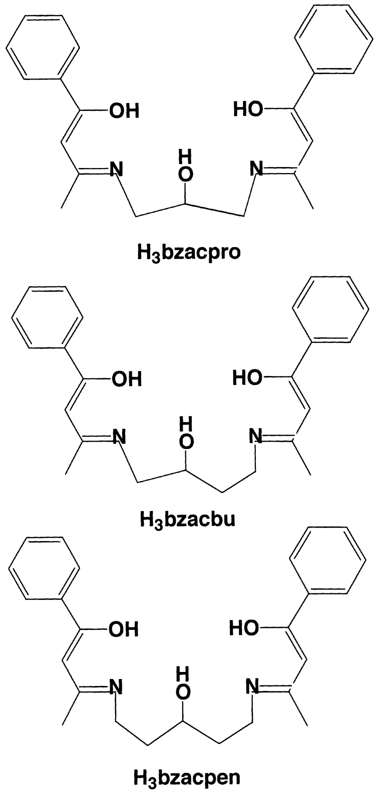

Scheme 1.

(8 cm^3). The mixed solution was refluxed for 2 h, and then allowed to stand overnight at 5 °C. The resulting pale-brown crystals were filtered, washed with diethyl ether and dried in vacuo over P_2O_5. Yield, 0.91 g (46%). Found: C, 73.30; H, 7.35; N, 7.40%. Calcd for $C_{24}H_{28}N_2O_3$: C, 73.44; H, 7.19; N, 7.14%. IR (KBr) ν(C=O) 1595 (s), ν(C=C) 1575 (s), 1537 (s), 1433, 1323, 1288 cm^{-1}.

***N,N′*-Bis(1-methyl-3-hydroxy-3-phenyl-2-propen-1-ylidene)-1,5-diamino-3-pentanol (H_3bzacpen).** 1,5-Diamino-3-pentanol (2.37 g, 20.0 mmol) was dissolved in methanol (10 cm^3) and added to a solution of benzoylacetone (6.49 g, 40.0 mmol) in methanol (10 cm^3). The mixed solution was refluxed for 2 h and then allowed to stand overnight at 5 °C. The resulting white crystals were filtered, washed with diethyl ether and dried in vacuo over P_2O_5. Yield, 1.30 g (15.0%). Found: C, 73.60; H, 7.60; N, 7.03%. Calcd for $C_{25}H_{30}N_2O_3$: C, 73.86; H, 7.44; N, 6.89%. IR (KBr) ν(C=O) 1595 (s), ν(C=C) 1575 (s), 1538 (s), 1431, 1376, 1321, 1289 cm^{-1}.

Synthesis of the Complexes. [Cu_2(bzacpro)(CH_3CO_2)] (1). After H_3bzacpro (19 mg, 0.05 mmol) was dissolved in acetonitrile (5 cm^3), a solution of copper(II) acetate monohydrate (18 mg, 0.10 mmol) in acetonitrile (5 cm^3) was added. After the mixed solution was allowed to stand for several days at room temperature, deep-blue plates resulted, which were filtered and dried in vacuo over P_2O_5: Yield, 16 mg (57%). Found: C, 53.33; H, 4.59; N, 5.36%. Calcd for $C_{25}H_{26}Cu_2N_2O_5$: C, 53.47; H, 4.67; N, 4.99%. IR (KBr) ν(C=C) 1590 (s), $\nu_{as}(COO^-)$ 1574 (s), ν(C=N) 1503 (s), 1480 (s), 1460 (s), 1420 (s), $\nu_s(COO^-)$ 1412 cm^{-1} (s). μ_{eff} (300 K) per Cu_2 dimer/μ_B 2.14. λ_M (CH_2Cl_2) 0 S mol^{-1} cm^2. Diffuse reflectance spectrum: λ_{max}/nm 243, 275, 332, 609. Electronic spectrum in CH_2Cl_2 λ_{max}/nm (ε per Cu/dm^3 mol^{-1} cm^{-1}) 241 (14300), 278 (8340), 347 (14900), 612 (215).

[Cu_4(bzacpro)$_2$(C_2H_5O)$_2$] (2). After H_3bzacpro (19 mg, 0.05 mmol) and copper(II) chloride dihydrate (17 mg, 0.10 mmol) were dissolved in ethanol (2.5 cm^3)–acetonitrile (7.5 cm^3), triethylamine (65 mg, 0.64 mmol) was added. After the mixed solution was allowed to stand for several days at room temperature, dark-green plates resulted, which were filtered and dried in vacuo over P_2O_5: Yield, 15 mg (55%). Found: C, 54.67; H, 5.24; N, 5.36%. Calcd for $C_{50}H_{56}Cu_4N_4O_8$: C, 54.83; H, 5.15; N, 5.12%. IR (KBr) ν(C=C) 1595, 1571, ν(C=N) 1506 (s), 1481 (s), 1455 (s), 1410 cm^{-1} (s). μ_{eff} (300 K) per Cu_4 tetramer/μ_B 3.66. λ_M (CH_2Cl_2) 0 S mol^{-1} cm^2. Diffuse reflectance spectrum: λ_{max}/nm 235, 287, 318, 404, 650. Electronic spectrum in CH_2Cl_2: λ_{max}/nm (ε per Cu /dm^3 mol^{-1} cm^{-1}) 242 (14700), 297 (7970), 348 (13100), 658 (163).

[Cu_2(bzacbu)(CH_3CO_2)] (3). After H_3bzacbu (20 mg, 0.05 mmol) was dissolved in acetonitrile (5 cm^3), a solution of copper(II) acetate monohydrate (18 mg, 0.10 mmol) in acetonitrile (5 cm^3) was added. After the mixed solution was allowed to stand for several days at room temperature, dark-green plates resulted, which were filtered and dried in vacuo over P_2O_5: Yield, 20 mg (69%). Found: C, 54.33; H, 4.95; N, 4.94%. Calcd for $C_{26}H_{28}Cu_2N_2O_5$: C, 54.25; H, 4.90; N, 4.87%. IR (KBr) ν(C=C) 1593, 1565 (s), $\nu_{as}(COO^-)$ 1570 (s), ν(C=N) 1501 (s), 1482 (s), 1452 (s), $\nu_s(COO^-)$ 1413 cm^{-1} (s). μ_{eff} (300 K) per Cu_2 dimer/μ_B 2.17. λ_M (CH_2Cl_2) 0 S mol^{-1} cm^2. Diffuse reflectance spectrum: λ_{max}/nm 233, 275, 317, 385sh, 618. Electronic spectrum in CH_2Cl_2: λ_{max}/nm (ε per Cu/dm^3 mol^{-1} cm^{-1}) 244 (16600), 280 (8150), 347 (15000), 618 (153).

[Cu_4(bzacbu)$_2$(CH_3O)$_2$] (4). After H_3bzacbu (20 mg, 0.05 mmol) was dissolved in methanol (5 cm^3), a solution of copper(II) perchlorate hexahydrate (37 mg, 0.10 mmol) in methanol (5 cm^3) was added, followed by triethylamine (35 mg, 0.10 mmol) with stirring. After the solution had been filtered, the filtrate was placed at room temperature for several days to give dark-green plates. Yield, 15 mg (55%). Found: C, 55.18; H, 4.94; N, 5.15%. Calcd for $C_{50}H_{56}Cu_4N_4O_8$: C, 54.83; H, 5.15; N, 5.12%. IR (KBr) ν(C=C) 1595, 1571, ν(C=N) 1507 (s), 1481 (s), 1455 (s), 1413 cm^{-1} (s). μ_{eff} (300 K) per Cu_4 tetramer/μ_B 3.20. λ_M (CH_2Cl_2) 0 S mol^{-1} cm^2. Diffuse reflectance spectrum: λ_{max}/nm 232, 285sh, 322, 385sh, 655. Electronic spectrum in CH_2Cl_2: λ_{max}/nm (ε per Cu/dm^3 mol^{-1} cm^{-1}) 245 (14600), 275 (6350), 350 (20600), 642 (79).

[Cu_4(bzacpen)$_2$(CH_3CO_2)$_2$] (5). After H_3bzacpen (10 mg, 0.03 mmol) was dissolved in acetonitrile (9 cm^3), a solution of copper(II) acetate monohydrate (18 mg, 0.10 mmol) in acetonitrile (9 cm^3) was added. The mixed solution was left standing for several days at room temperature to give dark-green plates. These were collected by filtration and dried in vacuo over P_2O_5: Yield, 10 mg (68%). Found: C, 54.90; H, 5.12; N, 4.92%. Calcd for $C_{54}H_{60}Cu_4N_4O_{10}$: C, 55.00; H, 5.13; N, 4.75%. IR (KBr) $\nu_{as}(COO^-)$ 1675 (s), ν(C=C) 1588 (s), 1564 (s), ν(C=N) 1510 (s), 1483 (s), 1458 (s), 1412 (s), $\nu_s(COO^-)$ 1354 cm^{-1} (s). μ_{eff} (300 K) per Cu_4 tetramer/μ_B 2.52. λ_M (CH_2Cl_2) 0 S mol^{-1} cm^2. Diffuse reflectance spectrum: λ_{max}/nm 318, 400sh, 655. Electronic spectrum in CH_2Cl_2 λ_{max}/nm (ε per Cu/dm^3 mol^{-1} cm^{-1}) 247 (18300), 351 (16900), 566 (99).

[Cu_4(bzacpen)$_2$O]·H_2O (6). After H_3bzacpen (10 mg, 0.03 mmol) and copper(II) chloride dihydrate (9 mg, 0.05 mmol) were dissolved in acetonitrile (10 cm^3), triethylamine (39 mg, 0.38 mmol) was added. After the mixed solution was allowed to stand for several days at room temperature, dark-greenish-brown plates resulted, which were filtered and dried in vacuo over P_2O_5: Yield, 8 mg (58%). Found: C, 54.73; H, 5.01; N, 5.23%. Calcd for $C_{50}H_{56}Cu_4N_4O_8$: C, 54.83; H, 5.15; N, 5.12%. IR (KBr) ν(C=C) 1589, 1566, ν(C=N) 1507 (s), 1482 (s), 1458 (s), 1410 cm^{-1} (s). $\mu_{\rm eff}$ (300 K) per Cu_4 tetramer/μ_B 2.98. λ_M (CH_2Cl_2) 0 S mol^{-1} cm^2. Diffuse reflectance spectrum: $\lambda_{\rm max}$/nm 232, 317, 380sh, 575. Electronic spectrum in CH_2Cl_2: $\lambda_{\rm max}$/nm (ε per Cu/dm^3 mol^{-1} cm^{-1}) 247 (16600), 352 (14900), 570 (80).

Measurements. Carbon, hydrogen, and nitrogen analyses were carried out using a Perkin-Elmer 2400 Series II CHNS/O Analyzer. Infrared spectra were measured with a JASCO Infrared Spectrophotometer model IR700 in the 4000–400 cm^{-1} region on a KBr disk. The electronic conductivities were measured on a Horiba conductivity meter (DS-14). Electronic spectra were measured with a Shimadzu UV-vis-NIR Recording Spectrophotometer (Model UV-3100). The temperature dependence of the magnetic susceptibilities was measured with a Quantum Design MPMS-5S SQUID susceptometer operating at a magnetic field of 0.5 T between 4 and 300 K. The susceptibilities were corrected for the diamagnetism of the constituent atoms using Pascal's constants.[37] The effective magnetic moments were calculated from the equation $\mu_{\rm eff} = 2.828\sqrt{\chi_M T}$, where χ_M is the magnetic susceptibility per mole.

X-ray Crystal Structure Analysis. Diffraction data were collected on an Enraf-Nonius CAD4 diffractometer using graphite-monochromated Mo-$K\alpha$ radiation at 25 ± 1 °C. Crystal data and details of the data collection are given in Table 1. The unit-cell parameters were determined by a least-squares refinement based on 25 reflections with $20 \le 2\theta \le 30°$. Intensity data were corrected for Lorentz-polarization effects. The structures were solved by direct methods and refined by full-matrix least-squares methods. All of the non-hydrogen atoms were refined with anisotropic thermal parameters. In the case of H_3bzacpro, hydrogen atoms attached to the alkoxy-oxygen and amino-nitrogen atoms were located from a difference Fourier map, and the other hydrogen atoms were inserted at their calculated positions. These hydrogen atoms were fixed at their positions. Hydrogen atoms of H_3bzacbu and H_3bzacpen were located from the difference Fourier maps and fixed at their positions. For **1**–**6**, hydrogen atoms were inserted at their calculated positions and fixed at their positions. The final discrepancy factors, $R = \Sigma||F_o| - |F_c|| / \Sigma|F_o|$, $R_w = [\Sigma w(|F_o| - |F_c|)^2/ \Sigma w|F_o|^2]^{1/2}$, are listed in Table 1. The weighting scheme, $w = 1/[\sigma^2(|F_o|) + (0.02|F_o|)^2 + 1.0]$, was employed. All of the calculations were carried out on a VAX station 4000 90A computer using a MolEN program package.[38] The atomic coordinates and thermal parameters of the atoms and the anisotropic thermal parameters of the non-hydrogen atoms have been deposited as Document No. 75050 at the Office of the Editor of Bull. Chem. Soc. Jpn. Crystallographic data have been deposited at the CCDC, 12 Union Road, Cambridge CB2 1EZ, UK and copies can be obtained on request, free of charge, by quoting the publication citation and the deposition numbers 193370–193378.

Results and Discussion

The present Schiff-base ligands were synthesized by a one-pot reaction from benzoylacetone under a condition [reflux with half amount of diamine (1,3-diamino-2-propanol, 1,4-diamino-2-butanol, and 1,5-diamino-3-pentanol) in methanol for several hours] similar to those we previously reported for the corresponding salicylideneaminate ligands.[28] Although bzacpro^{3-} is commonly found as a constituent of alkoxo-bridged metal complexes,[32,36] little information is available on the structure of the free ligand H_3bzacpro. To elucidate the structures of the free Schiff-base ligands, a crystal-structure determination was performed not only for H_3bzacpro, but also for H_3bzacbu and H_3bzacpen. The crystal structure of the H_3bzacpro ligand is shown in Fig. 1. In the crystal, the ligand does not take a planar structure, but an extended form, showing a twisting of the two side arms around the central alkoxy group. The C–O bands [O1–C7 1.237(9), O2–C17 1.243(9) Å] are in the normal observed bond lengths of C=O bonds; the C=N imine bonds [N1–C9 1.335(9) and N2–C15 1.308(1) Å] are a little longer than the normal C=N imine bond lengths, although these distances are significantly shorter than the C–N bond lengths [N1–C11 1.445(10), N2–C13 1.457(9) Å]. Moreover, hydrogen atoms are attached to the N1 and N2 atoms. These facts show that the Schiff-base is in a keto-amine tautomer. There are intramolecular hydrogen bonds between them [O1···H(N1) 1.644 Å, O1···H(N1)–N1 141.5°, O2···H(N2) 2.043 Å, O2···H(N2)–N2 134.4°]. One of the two keto groups of H_3bzacpro is hydrogen-bonded to the alkoxy group of the neighboring Schiff-base ligand [O2···H(O3)′ 1.707 Å, O2···H(O3)′–O3′ 168.5°], forming a dimer of H_3bzacpro in the crystal.

The crystal structure of H_3bzacbu is shown in Fig. 2. The molecule has an extended *trans* form having a crystallographic inversion center at the midpoint of C12–C12′. The alkoxy group is disordered and distributed into the two positions O2 and O2′ with an occupancy factor of 0.5, respectively. The O1–C7 and N–C9 distances are 1.267(3) and 1.328(4) Å, respectively, which are consistent with the keto-amine tautomer. There is an intramolecular hydrogen bond [O1···H(N) 1.793 Å, O1···H(N)–N 135.9°] and an intermolecular hydrogen bond between the keto and the alkoxy group of the

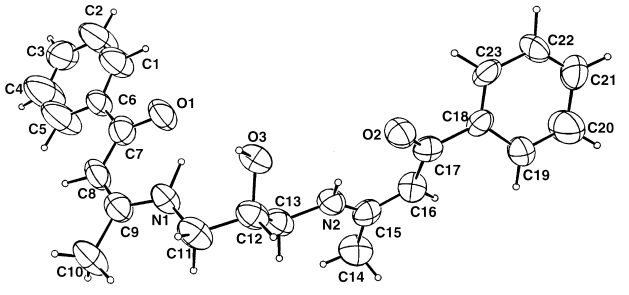

Fig. 1. ORTEP drawing of the structure of H_3bzacpro, showing the atom-labeling scheme. Thermal ellipsoids are at the 50% probability.

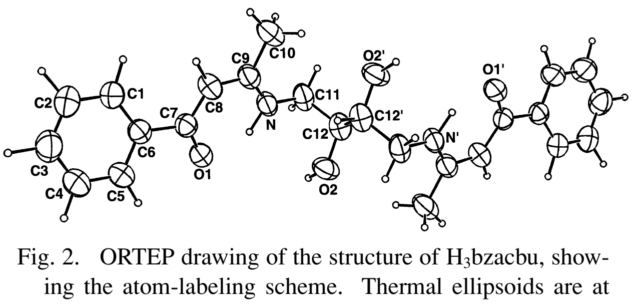

Fig. 2. ORTEP drawing of the structure of H_3bzacbu, showing the atom-labeling scheme. Thermal ellipsoids are at the 50% probability.

Table 1. Crystal Data and Data Collection Details

Complex	H_3bzacpro	H_3bzacbu	H_3bzacpen	[Cu_2(bzacpro)-(CH_3CO_2)](**1**)	[Cu_4(bzacpro)$_2$-(C_2H_5O)$_2$](**2**)	[Cu_2(bzacbu)-(CH_3CO_2)](**3**)	[Cu_4(bzacbu)-(CH_3O)$_2$](**4**)	[Cu_4(bzacpen)$_2$-(CH_3CO_2)$_2$](**5**)	[Cu_4(bzacpen)$_2$O]·H_2O (**6**)
Formula	$C_{23}H_{26}N_2O_3$	$C_{24}H_{28}N_2O_3$	$C_{25}H_{30}N_2O_3$	$C_{25}H_{26}Cu_2N_2O_5$	$C_{50}H_{56}Cu_4N_4O_8$	$C_{26}H_{28}Cu_2N_2O_5$	$C_{50}H_{56}Cu_4N_4O_8$	$C_{54}H_{60}Cu_4N_4O_{10}$	$C_{50}H_{56}Cu_4N_4O_8$
Fw	378.5	392.5	406.5	561.6	1095.2	575.6	1095.2	1179.3	1095.2
Crystal system	monoclinic	monoclinic	triclinic	monoclinic	monoclinic	triclinic	monoclinic	monoclinic	monoclinic
Space group	$C2/c$	$P2_1/a$	$P\bar{1}$	$C2/c$	$P2_1/n$	$P\bar{1}$	$P2_1/n$	$P2_1/c$	$C2/c$
a/Å	36.371(11)	11.558(6)	8.819(2)	22.382(9)	10.071(3)	17.316(9)	22.374(8)	14.916(4)	22.866(17)
b/Å	5.325(1)	8.091(2)	9.447(3)	8.179(2)	12.747(7)	18.801(10)	8.558(2)	9.509(2)	14.333(3)
c/Å	21.643(7)	12.275(6)	15.600(5)	27.932(11)	18.694(5)	8.347(4)	27.593(11)	17.756(4)	14.079(11)
α/°			83.64(2)			102.77(3)			
β/°	92.09(1)	108.05(2)	74.83(2)	109.70(2)	99.61(1)	103.90(3)	113.05(1)	101.17(1)	97.02(4)
γ/°			62.98(3)			101.54(3)			
V/Å^3	4189(2)	1088.6(8)	1117.4(7)	4814(3)	2366(1)	2479(2)	4862(3)	2470.5(9)	4580(5)
Z	8	2	2	8	2	4	4	2	4
D_c/g cm^{-3}	1.20	1.20	1.21	1.55	1.54	1.54	1.50	1.59	1.59
D_m/g cm^{-3}	1.21	1.18	1.22	1.60	1.55	1.55	1.46	1.59	1.57
μ(Mo $K\alpha$)/cm^{-1}	0.74	0.74	0.74	18.09	18.35	17.58	17.86	17.66	18.96
Crystal size/mm	0.15 × 0.30 × 0.60	0.30 × 0.45 × 0.62	0.15 × 0.62 × 0.65	0.20 × 0.40 × 0.45	0.20 × 0.20 × 0.22	0.22 × 0.45 × 0.54	0.26 × 0.38 × 0.50	0.35 × 0.48 × 0.50	0.15 × 0.28 × 0.55
2θ range/°	2.0–48.0	2.0–48.0	2.0–48.0	2.0–46.0	2.0–48.0	2.0–48.0	2.0–46.0	2.0–48.0	2.0–50.0
Total no. of reflections measured	3690	1841	3482	3609	3905	7781	7315	4134	4186
No. of unique reflections with $I \geq 3\sigma(I)$	1060	969	2130	1792	1943	5838	2988	3148	2409
R	0.061	0.049	0.070	0.047	0.044	0.078	0.051	0.039	0.063
R_w	0.064	0.054	0.078	0.052	0.050	0.090	0.056	0.046	0.073

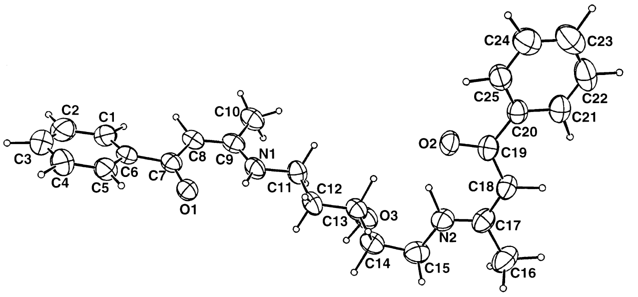

Fig. 3. ORTEP drawing of the structure of H_3bzacpen, showing the atom-labeling scheme. Thermal ellipsoids are at the 50% probability.

neighboring Schiff-base ligand [O1···H(O2)″ 1.468 Å, O1···H(O2)″–O2″ 156.5°].

As shown in Fig. 3, the Schiff-base ligand H_3bzacpen consists of discrete molecules in the keto-amine tautomer [O1–C7 1.263(6), O2–C19 1.247(8), N1–C9 1.319(7), N2–C17 1.321(9) Å] with intramolecular hydrogen bonds [O1···H(N1) 2.000, O2···H(N2) 1.740 Å, O1···H(N1)–N1 126.0, O2···H(N2)–N2 130.0°] The two side arms have a severely twisted conformation. The molecule is associated with the neighboring molecule by intermolecular hydrogen bondings [O1···H(O3′) 1.814 Å, O1···H(O3)′–O3′ 159.7°].

The present Schiff-base ligands show ν(C=O) and ν(C=C) bands of the benzoylacetonato moiety at 1598–1595 and 1578–1535 cm^{-1}, respectively, in the infrared spectra, which are consistent with the keto-amine tautomer of the benzoylacetoneimine moiety.

The present complexes were prepared via the one-pot synthesis describing in the Experimental Section. In previous papers, we reported that the H_3bzacpro ligand affords the mononuclear species [Pd(Hbzacpro)],[36d] dinuclear species $[(VO)_2\text{-(bzacpro)(pz)}]$ (Hpz = pyrazol),[36e] trinuclear species $[Mn_3\text{-(bzacpro)}_2(CH_3O)_2(CH_3OH)(C_2H_5OH)](ClO_4)$,[36a] tetranuclear species $[Co_4(\text{bzacpro})_2(CH_3O)_4]$,[36b] $[Co_4(\text{bzacpro})_2\text{-}(C_2H_5O)_4]$,[36b] $[Zn_4(\text{Hbzacpro})_4]$,[36c] $[Ni_4(\text{bzacpro})_2(CH_3O)_2\text{-}(CH_3OH)_2]$,[36f] $[Ni_2Zn_2(\text{bzacpro})_2(CH_3O)_2(CH_3OH)_2]$[36c] and octanuclear species $[Zn_8(\text{bzacpro})_4(OH)_4]$.[36c] In the present cases, the reaction of the Schiff-base ligand with copper(II) gave dinuclear and tetranuclear species $[Cu_2(\text{bzacpro})(CH_3CO_2)]$ (**1**) and $[Cu_4(\text{bzacpro})_2(C_2H_5O)_2]$ (**2**), depending on the exogenous ligand, which comes from the metal source or solvent. The H_3bzacbu ligand also affords similar dinuclear and tetranuclear species $[Cu_2(\text{bzacbu})(CH_3CO_2)]$ (**3**) and $[Cu_4\text{-}(\text{bzacbu})_2(CH_3O)_2]$ (**4**). On the other hand, the H_3bzacpen ligand affords only the tetranuclear species $[Cu_4(\text{bzacpen})_2\text{-}(CH_3CO_2)_2]$ (**5**) and $[Cu_4(\text{bzacpen})_2O]\cdot H_2O$ (**6**).

The X-ray crystallography of **1** reveals a dinuclear structure where two copper(II) ions are bridged by the alkoxo-oxygen atom of the Schiff-base ligand bzacpro and the exogenous acetate ion in a *syn–syn* configuration. A perspective view of the molecule is shown in Fig. 4. Selected bond distances and angles are listed in Table 2. Each copper atom takes a planar geometry with keto-oxygen, amino-nitrogen, and alkoxo-oxygen donor atoms of bzacpro and acetate ion. The Cu1–Cu2 distance and Cu1–O3–Cu2 angle are 3.498(1) Å and 131.8(3)°, respectively. A similar dinuclear structure was already known in the literature.[22,24,31] Contrary to the structure of the free ligand, the 1,3-diamino-propane backbone of bzacpro in **1** takes a planar structure, resulting in a coplanar structure of the two coordination spheres. The dihedral angle of the two coordination planes is 174.5°. In the crystal, the two planar dinuclear molecules are stacked on each other with a close Cu2–Cu2′ distance of 3.570(2) Å (Fig. 5).

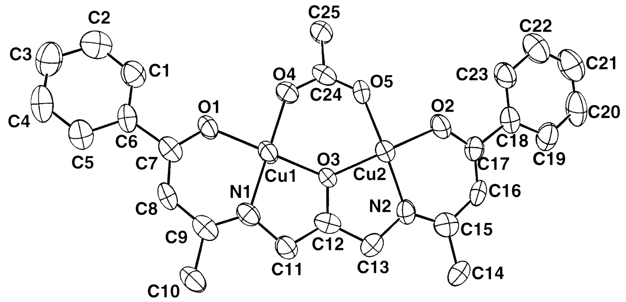

Fig. 4. ORTEP drawing of the structure of $[Cu_2(\text{bzacpro})\text{-}(CH_3CO_2)]$ (**1**) showing the 35% probability thermal ellipsoids and atom labeling scheme. Hydrogen atoms are omitted for clarity.

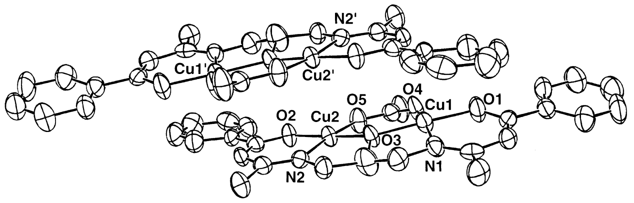

Fig. 5. View of the stacking feature of $[Cu_2(\text{bzacpro})\text{-}(CH_3CO_2)]$ (**1**).

The crystal structure of **3** consists of crystallographically independent dinuclear molecules, which are similar to that of **1** (Fig. 6). In these dinuclear molecules, the aliphatic backbones of bzacpro are not planar, and the dihedral angles of the two coordination planes within the dinuclear molecules are both 136.5°. The Cu1–Cu2 and Cu3–Cu4 distances are both 3.393(1) Å. The Cu1–O3–Cu2 and Cu3–O8–Cu4 angles are 125.1(4) and 125.3(3)°, respectively. In the infrared spectra of **1** and **3**, the antisymmetric and symmetric C–O stretching bands of the acetate ions are found at around 1570 and 1410 cm^{-1}, respectively. This feature is in harmony with the *syn–syn* bridging mode of the acetate group.[39]

The crystal structure of **5** is shown in Fig. 7. The tetranuclear molecule is crystallographically centrosymmetric. The two Cu atoms are bridged by an alkoxo-oxygen atom (O3) of the Schiff-base ligand bzacpen and an oxygen atom (O4) of an acetate group with a monatomic bridging mode. The Cu1–Cu2 distance and Cu1–O3–Cu2 angle are 3.049(1) Å and 106.6(1)°, respectively. The shortening of the Cu–Cu distance and the acute Cu–O–Cu angle compared with those of **1** and **3** may be caused by the steric requirement of the adjacent 6-6-membered chelate rings of the ligand backbone of bzacpen^{3-}. The various bridging modes of acetate ion in **1**, **3**, and **5** means the flexible coordinating properties of the acetate ion.[40] The two alkoxo-bridged dinuclear units are held together by further bridging of the monatomic bridging acetate ion (O4 and O4′)

Table 2. Selected Bond Distances (Å) and Angles (°) with Their Estimated Standard Deviations in Parentheses

H_3bzacpro				$[Cu_2(bzacpro)(CH_3CO_2)]$ (**1**)				Cu4–Cu4′	3.318(2)	Cu2–O4	1.931(6)
O1–C7	1.237(9)	C12–C13	1.489(11)	Cu1–Cu2	3.498(1)	Cu1–N1	1.909(8)	Cu1–O1	1.883(7)	Cu2–N2	1.938(8)
O2–C17	1.243(9)	C14–C15	1.492(12)	Cu2–Cu2′[d]	3.570(2)	Cu2–O2	1.896(6)	Cu1–O3	1.913(7)	Cu3–O5	1.875(8)
O3–C12	1.428(10)	C15–C16	1.397(10)	Cu1–O1	1.893(6)	Cu2–O3	1.910(6)	Cu3–O7	1.901(8)	Cu4–O7	1.946(6)
N1–C9	1.335(9)	C16–C17	1.397(11)	Cu1–O3	1.922(5)	Cu2–O5	1.942(6)	Cu3–O8	1.945(6)	Cu4–O7′	2.535(7)
N1–C11	1.445(10)	C17–C18	1.506(10)	Cu1–O4	1.925(7)	Cu2–N2	1.918(7)	Cu3–N3	1.938(9)	Cu4–O8	1.916(8)
N2–C13	1.457(9)	O1–H(N1)	1.644	Cu1–O3–Cu2	131.8(3)	O2–Cu2–O3	177.9(3)	Cu4–O6	1.921(6)	Cu4–N4	1.930(10)
N2–C15	1.308(10)	O2–H(O3)′[a]	1.707	O1–Cu1–O3	179.2(3)	O2–Cu2–O5	85.3(3)	O1–Cu1–O3	170.0(4)	O7–Cu3–N3	90.5(4)
C6–C7	1.500(11)	O2–H(N2)	2.043	O1–Cu1–O4	85.6(3)	O2–Cu2–N2	94.8(3)	O1–Cu1–O4	96.4(4)	O8–Cu3–N3	161.3(3)
C7–C8	1.425(12)	O3–H(O3)	1.018	O1–Cu1–N1	94.5(3)	O3–Cu2–O5	95.5(3)	O1–Cu1–N1	98.8(4)	O6–Cu4–O7	173.9(3)
C8–C9	1.347(11)	N1–H(N1)	1.160	O3–Cu1–O4	94.8(3)	O3–Cu2–N2	84.6(3)	O3–Cu1–O4	79.4(3)	O6–Cu4–O7′	90.6(3)
C9–C10	1.514(13)	N2–H(N2)	0.803	O3–Cu1–N1	85.1(3)	O5–Cu2–N2	173.5(3)	O3–Cu1–N1	87.6(4)	O6–Cu4–O8	97.8(3)
C11–C12	1.506(11)			O4–Cu1–N1	169.4(3)			O4–Cu1–N1	159.7(4)	O6–Cu4–N4	95.4(3)
C9–N1–C11	127.6(7)	O2–C17–C16	123.0(6)					O2–Cu2–O3	171.6(3)	O7–Cu4–O7′	85.4(2)
C13–N2–C15	128.2(6)	O2–C17–C18	118.0(6)	$[Cu_4(bzacpro)_2(C_2H_5O)_2]$ (**2**)				O2–Cu2–O3″	93.1(3)	O7–Cu4–O8	78.0(3)
O1–C7—C6	117.0(7)	C16–C17–C18	119.0(6)	Cu1–Cu1′[e]	3.256(1)	Cu1–O4′	2.443(5)	O2–Cu2–O4	94.5(3)	O7–Cu4–N4	89.8(3)
O1–C7—C8	124.1(7)	O12–O3–H(O3)	108.9	Cu1–Cu2	3.073(1)	Cu1–N1	1.930(7)	O2–Cu2–N2	95.9(4)	O7′–Cu4–O8	93.8(3)
N1–C9—C8	122.5(7)	C9–N1–H(N1)	106.5	Cu1–Cu2′	3.262(1)	Cu2–O1′	2.666(6)	O3–Cu2–O3″	83.8(3)	O7′–Cu4–N4	98.9(3)
N1–C9—C10	116.8(7)	C11–N1–H(N1)	125.6	Cu2–Cu2′	5.438(2)	Cu2–O2	1.906(6)	O3–Cu2–O4	77.9(3)	O8–Cu4–N4	161.6(4)
C8–C9—C10	120.7(7)	C13–N2–H(N2)	114.2	Cu1–O1	1.921(6)	Cu2–O3	1.959(5)	O3–Cu2–N2	92.3(4)	Cu1–O3–Cu2	99.6(3)
N2–C15–C14	117.4(6)	C15–N2–H(N2)	117.6	Cu1–O3	1.961(6)	Cu2–O4′	1.949(5)	O3″–Cu2–O4	93.3(3)	Cu1–O3–Cu2″	105.4(3)
N2–C15–C16	121.4(7)	O2–H(O3)′–O3′	168.5	Cu1–O4	1.967(5)	Cu2–N2	1.942(7)	O3″–Cu2–N2	97.9(4)	Cu2–O3–Cu2″	96.2(3)
C14–C15–C16	121.2(7)	O1–H(N1)–N1	141.5	O1–Cu1–O3	174.9(2)	O1–Cu1–O4	87.5(2)	O4–Cu2–N2	164.3(4)	Cu1–O4–Cu2	100.5(3)
C15–C16–C17	124.4(7)	O2–H(N2)–N2	134.4	O1–Cu1–O4′	100.3(2)	O2–Cu2–O4′	94.3(2)	O5–Cu3–O7	168.7(3)	Cu3–O7–Cu4	101.1(3)
				O1–Cu1–N1	94.5(3)	O2–Cu2–N2	93.2(3)	O5–Cu3–O8	96.9(3)	Cu3–O7–Cu4′	104.2(3)
H_3bzacbu				O3–Cu1–O4	93.8(2)	O3–Cu2–O4′	87.7(2)	O5–Cu3–N3	96.7(4)	Cu4–O7–Cu4′	94.6(3)
O1–C7	1.267(3)	C9–C10	1.501(5)	O3–Cu1–O4′	75.0(2)	O3–Cu2–N2	84.4(3)	O7–Cu3–O8	78.4(3)	Cu3–O8–Cu4	100.6(4)
O2–C12	1.418(6)	C11–C12	1.538(5)	O3–Cu1–N1	85.3(3)	O4′–Cu2–N2	166.4(3)				
N–C9	1.328(4)	C12–C12′[b]	1.499(5)	O4–Cu1–O4′	85.4(2)	Cu1–O1–Cu2′	89.1(2)	$[Cu_4(bzacpen)_2(CH_3CO_2)_2]$ (**5**)			
N–C11	1.455(4)	O1–H(O2)″[b]	1.468	O4–Cu1–N1	166.6(2)	Cu1–O3–Cu2	103.3(2)	Cu1–Cu1′[g]	5.412(1)	Cu1–O4	2.057(3)
C6–C7	1.498(4)	O1–H(N)	1.793	O4′–Cu1–N1	107.2(2)	Cu1–O4–Cu1′	94.6(2)	Cu1–Cu2	3.049(1)	Cu1–N1	1.948(4)
C7–C8	1.413(5)	O2–H(O2)	1.214	O1′–Cu2–O2	98.4(2)	Cu1–O4–Cu2′	112.9(3)	Cu1–Cu2′	3.380(1)	Cu2–O2	1.911(3)
C8–C9	1.383(5)	N–H(N)	1.061	O1′–Cu2–O3	84.8(2)	Cu1′–O4–Cu2′	88.1(2)	Cu2–Cu2′	3.486(1)	Cu2–O3	1.913(3)
C9–N–C11	128.3(3)	C8–C9–C10	119.2(3)	O1′–Cu2–O4′	69.3(2)	Cu1–O3–Cu2	103.3(2)	Cu1–O1	1.878(3)	Cu2–O4	2.114(2)
O1–C7–C6	118.3(3)	C12–O2–H(O2)	112.5	O1′–Cu2–N2	120.7(3)	Cu1–O4–Cu2′	112.9(3)	Cu1–O2′	2.588(3)	Cu2–O4′	2.339(3)
O1–C7—C8	122.5(3)	C9–N–H(N)	113.4	O2–Cu2–O3	176.7(2)			Cu1–O3	1.891(3)	Cu2–N2	1.943(3)
C6–C7—C8	119.2(2)	C11–N–H(N)	118.0					O1–Cu1–O2′	91.9(1)	O2–Cu2–N2	94.6(1)
C7–C8—C9	124.4(3)	O1–H(O2)″–O2″	156.5	$[Cu_2(bzacbu)(CH_3CO_2)]$ (**3**)				O1–Cu1–O3	160.6(1)	O3–Cu2–O4	78.7(1)
N–C9—C8	121.2(3)	O1–H(N)–N	135.9	Cu1–Cu2	3.393(1)	Cu2–N2	1.924(8)	O1–Cu1–O4	85.9(1)	O3–Cu2–O4′	102.0(1)
N–C9—C10	119.6(3)			Cu3–Cu4	3.393(1)	Cu3–O6	1.906(7)	O1–Cu1–N1	94.3(1)	O3–Cu2–N2	96.6(1)
				Cu1–O1	1.915(6)	Cu3–O8	1.925(7)	O2′–Cu1–O3	98.5(1)	O4–Cu2–O4′	77.1(1)
H_3bzacpen				Cu1–O3	1.929(6)	Cu3–O9	1.932(6)	O2′–Cu1–O4	76.7(1)	O4–Cu2–N2	165.9(1)
O1–C7	1.263(6)	O3–C13	1.442(7)	Cu1–O4	1.951(6)	Cu3–N3	1.923(7)	O2′–Cu1–N1	98.7(1)	O4′–Cu2–N2	117.0(1)

O2–C19	1.247(8)	N1–C9	1.319(7)	Cu1–N1	1.929(7)	Cu4–O7	1.910(5)	O3–Cu1–O4	80.6(1)	Cu1–O2′–Cu2′	96.2(1)
N1–C11	1.457(9)	C16–C17	1.521(7)	Cu2–O2	1.904(7)	Cu4–O8	1.894(5)	O3–Cu1–N1	100.3(1)	Cu1–O3–Cu2	106.6(1)
N2–C15	1.462(7)	C17–C18	1.372(7)	Cu2–O3	1.895(6)	Cu4–O10	1.978(7)	O4–Cu1–N1	175.4(1)	Cu1–O4–Cu2	93.9(1)
N2–C17	1.321(9)	C18–C19	1.441(6)	Cu2–O5	1.969(8)	Cu4–N4	1.924(8)	O2–Cu2–O3	161.6(1)	Cu1–O4–Cu2′	100.3(1)
C6–C7	1.505(9)	C19–C20	1.505(7)	O1–Cu1–O3	177.8(2)	O6–Cu3–O9	85.0(3)	O2–Cu2–O4	87.0(1)	Cu2–O4–Cu2′	102.9(1)
C7–C8	1.409(9)	O1–H(O3)′[c]	1.814	O1–Cu1–O4	84.8(3)	O6–Cu3–N3	93.5(3)	O2–Cu2–O4′	85.8(1)		
C8–C9	1.400(10)	O1–H(N1)	2.000	O1–Cu1–N1	93.4(3)	O8–Cu3–O9	92.8(3)				
C9–C10	1.505(9)	O2–H(N2)	1.740	O3–Cu1–O4	93.2(3)	O8–Cu3–N3	88.5(3)	[Cu$_4$(bzacpen)$_2$O]·H$_2$O (**6**)			
C11–C12	1.523(8)	O3–H(O3)	1.085	O3–Cu1–N1	88.5(3)	O9–Cu3–N3	172.3(3)	Cu1–Cu1′[h]	3.503(2)	Cu1–O4	1.950(5)
C12–C13	1.527(9)	N1–H(N1)	0.913	O4–Cu1–N1	172.1(3)	O7–Cu4–O8	160.5(3)	Cu1–Cu2	2.905(2)	Cu1–N1	1.955(9)
C13–C14	1.526(8)	N2–H(N2)	1.147	O2–Cu2–O3	159.9(2)	O7–Cu4–O10	85.0(3)	Cu1–Cu2′	2.923(2)	Cu2–O2	1.930(7)
C14–C15	1.509(10)			O2–Cu2–O5	85.5(3)	O7–Cu4–N4	93.8(3)	Cu2–Cu2′	3.734(1)	Cu2–O3	1.934(8)
C9–N1–C11	126.2(5)	C17–C18–C19	122.9(6)	O2–Cu2–N2	93.9(3)	O8–Cu4–O10	93.3(3)	Cu1–O1	1.917(6)	Cu2–O4	1.942(3)
C15–N2–C17	125.8(4)	O2–C19–C18	122.3(5)	O3–Cu2–O5	93.3(3)	O8–Cu4–N4	96.0(3)	Cu1–O3	1.891(7)	Cu2–N2	1.953(7)
O1–C7–C6	117.9(6)	O2–C19–C20	119.0(4)	O3–Cu2–N2	95.6(3)	O10–Cu4–N4	154.2(3)	O1–Cu1–O3	162.8(3)	O3–Cu2–O4	81.8(3)
O1–C7–C8	123.1(6)	C18–C19–C20	118.6(5)	O5–Cu2–N2	154.8(3)	Cu1–O3–Cu2	125.1(4)	O1–Cu1–O4	88.4(2)	O3–Cu2–N2	94.0(3)
C6–C7–C8	119.1(5)	C13–O3–H(O3)	106.0	O6–Cu3–O8	177.7(3)	Cu3–O8–Cu4	125.3(3)	O1–Cu1–N1	94.2(3)	O4–Cu2–N2	171.0(4)
C7–C8–C9	122.8(5)	C9–N1–H(N1)	122.5					O3–Cu1–O4	82.7(2)	Cu1–O3–Cu2	98.9(3)
N1–C9–C8	121.9(6)	C11–N1–H(N1)	110.4	[Cu$_4$(bzacbu)$_2$(CH$_3$O)$_2$] (**4**)				O3–Cu1–N1	96.6(3)	Cu1–O4–Cu1′	127.8(6)
N1–C9–C10	118.7(6)	C15–N2–H(N2)	119.1	Cu1–Cu2	2.931(2)	Cu1–O4	1.881(9)	O4–Cu1–N1	172.3(4)	Cu1–O4–Cu2	96.6(10)
C8–C9–C10	119.4(5)	C17–N2–H(N2)	113.8	Cu1–Cu2″[f]	3.556(2)	Cu1–N1	1.909(11)	O2–Cu2–O3	172.8(3)	Cu1–O4–Cu2′	97.4(10)
N2–C17–C16	118.3(5)	O1–H(O3)′–O3′	159.7	Cu2–Cu2″	3.341(1)	Cu2–O2	1.863(9)	O2–Cu2–O4	91.0(2)	Cu2–O4–Cu2′	148.0(6)
N2–C17–C18	122.0(5)	O1–H(N1)–N1	126.0	Cu3–Cu4	2.971(2)	Cu2–O3	1.924(9)	O2–Cu2–N2	93.2(3)		
C16–C17–C18	119.7(6)	O2–H(N2)–N2	130.3	Cu3–Cu4′[f]	3.523(2)	Cu2–O3″	2.532(8)				

a) Prime refers to the equivalent position $(1-x, 1-y, 1-z)$. b) Primes and double primes refer to the equivalent position $(1-x, 1-y, 2-z)$ and $(1-x, -y, 2-z)$, respectively. c) Prime refers to the equivalent position $(1-x, -1-y, -1-z)$. d) Prime refers to the equivalent position $(1/2-x, 3/2-y, -z)$. e) Prime refers to the equivalent position $(1-x, -y, 2-z)$. f) Primes and double primes refer to the equivalent position $(-x, 1-y, -z)$ and $(1-x, 2-y, 2-z)$, respectively. g) Prime refers to the equivalent position $(2-x, -y, 1-z)$. h) Prime refers to the equivalent position $(1-x, y, 1/2-z)$.

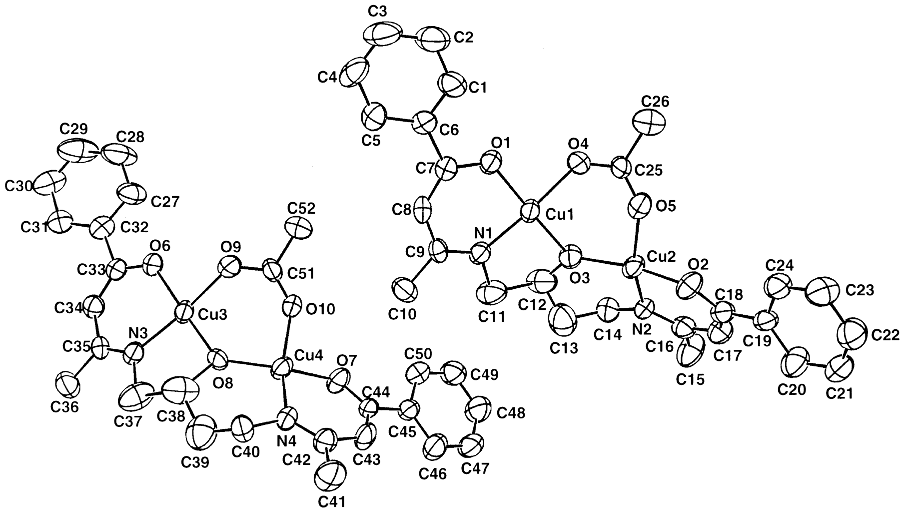

Fig. 6. ORTEP drawing of the structure of [Cu_2(bzacbu)(CH_3CO_2)] (**3**) showing the 35% probability thermal ellipsoids and atom labeling scheme. Hydrogen atoms are omitted for clarity.

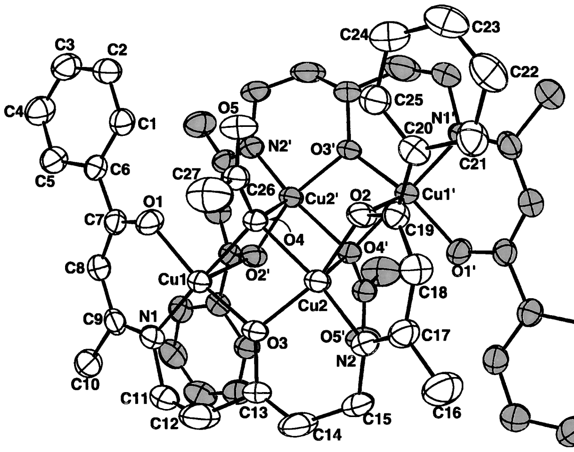

Fig. 7. ORTEP drawing of the structure of [Cu_4(bzacpen)$_2$-(CH_3CO_2)$_2$] (**5**) showing the 50% probability thermal ellipsoids and atom labeling scheme. Hydrogen atoms are omitted for clarity.

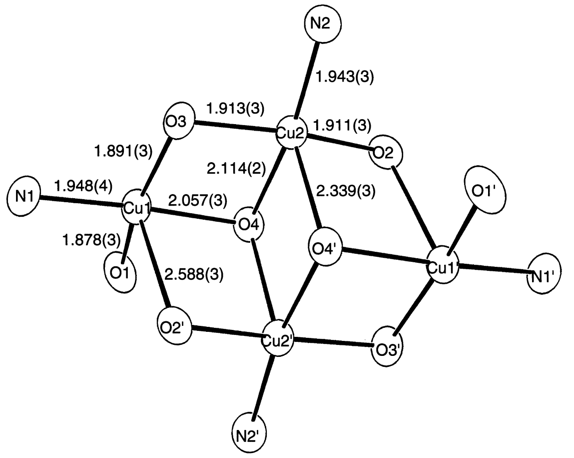

Fig. 8. Core structure of [Cu_4(bzacpen)$_2$(CH_3CO_2)$_2$] (**5**).

and keto-oxygen (O2 and O2′) to form a step-like tetranuclear core, as shown in Fig. 8. Each copper atom takes a distorted tetragonal-pyramidal geometry with an elongated axial Cu–O bond [Cu1–O2′ 2.588(3), Cu2–O4′ 2.339(3) Å]. The equatorial Cu–O bond lengths of Cu1–O3 [1.891(3) Å], Cu2–O3 [1.913(3) Å], Cu1–O4 [2.057(3) Å], and Cu2–O4 [2.114(2) Å] are significantly shorter than those of the axial Cu–O bonds. Therefore, the magnetic exchange interaction via Cu1–O3–Cu2 and Cu1–O4–Cu2 may be expected to contribute to the magnetic property of **5** predominantly. Only a few examples of structurally characterized copper(II) complexes with monatomic bridging of the acetate ion are known.[41]

The crystal structure of **2** is shown in Fig. 9. The tetranuclear molecule is crystallographically centrosymmetric. The Cu1 and Cu2 atoms are bridged by an alkoxo-oxygen atom (O3) of the Schiff-base ligand bzacpro and ethoxo ion (O4′). The two dinuclear units are associated into a step-to-step tetranuclear core (Fig. 10) by further bridging of keto-oxygen atoms (O1 and O1′) and ethoxo ions (O4 and O4′). The Cu1–O4′ and Cu2–O1′ lengths are 2.443(5) and 2.666(6) Å, respectively,

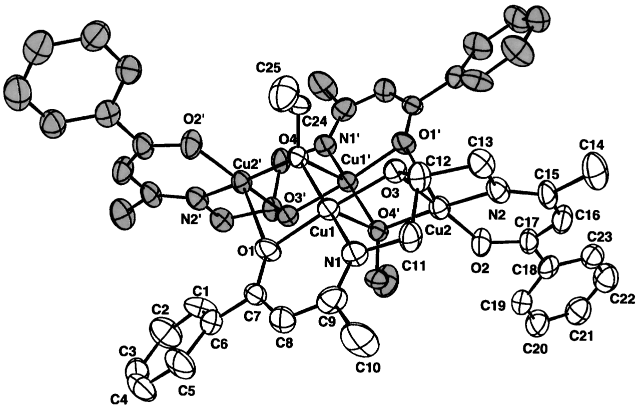

Fig. 9. ORTEP drawing of the structure of [Cu_4(bzacpro)$_2$-(C_2H_5O)$_2$] (**2**) showing the 35% probability thermal ellipsoids and atom labeling scheme. Hydrogen atoms are omitted for clarity.

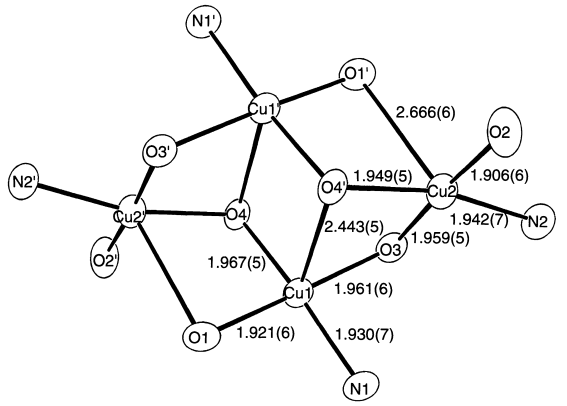

Fig. 10. Core structure of [$Cu_4(bzacpro)_2(C_2H_5O)_2$] (**2**).

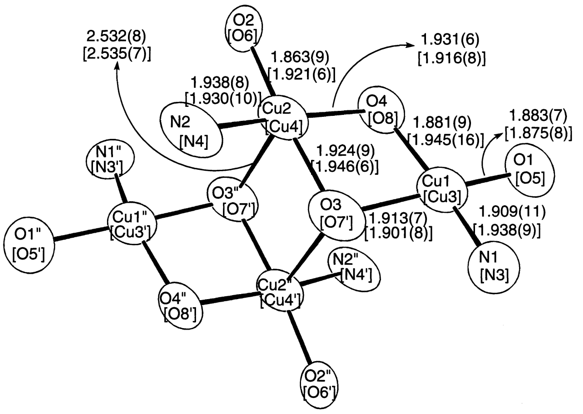

Fig. 12. Core structure of [$Cu_4(bzacbu)_2(CH_3O)_2$] (**4**).

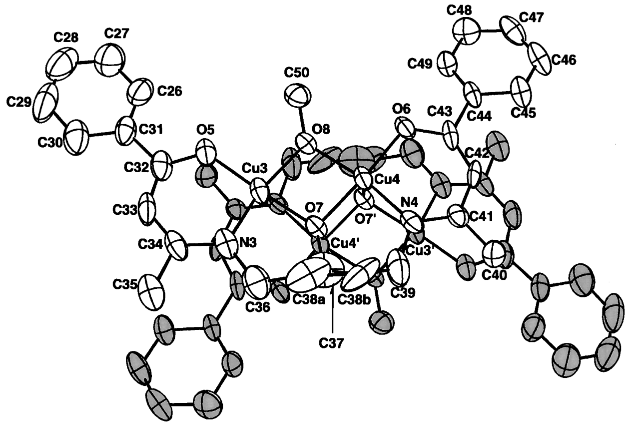

Fig. 11. ORTEP drawing of the structure (molecule b) of [$Cu_4(bzacbu)_2(CH_3O)_2$] (**4**) showing the 35% probability thermal ellipsoids and atom labeling scheme. Hydrogen atoms are omitted for clarity. Primed and unprimed atoms are related by the inversion.

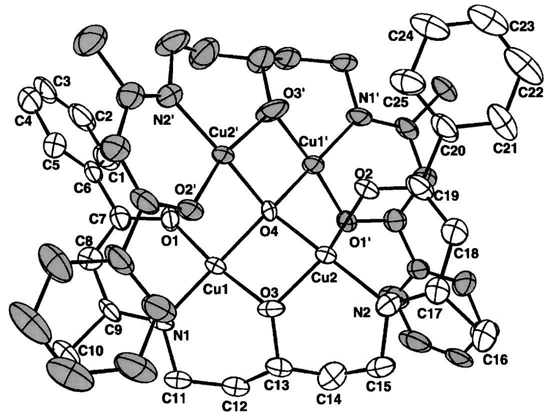

Fig. 13. ORTEP drawing of the structure of [$Cu_4(bzacpen)_2O$]·H_2O (**6**) showing the 35% probability thermal ellipsoids and atom labeling scheme. Hydrogen atoms and solvent molecule are omitted for clarity. Primed and unprimed atoms are related by the C_2 axis.

which are significantly longer than the Cu1–O3 [1.961(6) Å], Cu2–O3 [1.959(5) Å], Cu1–O4 [1.967(5) Å], and Cu2–O4′ [1.949(5) Å] lengths. Thus, the magnetic exchange coupling via Cu1–O3–Cu2 and Cu1–O4–Cu2′ may be important in this tetranuclear core. The Cu1–O3–Cu2 and Cu1–O4–Cu2′ angles are 103.3(2) and 112.9(3)°, respectively.

The crystal structure of **4** contains two crystallographically independent tetranuclear molecules, which have a crystallographic inversion center; they are abbreviated as a and b. Fig. 11 shows the structure of molecule b. Both comprise a similar centrosymmetric tetranuclear molecule, and no significant difference in the geometries can be recognized between molecules a and b. The tetranuclear core is shown in Fig. 12. The two μ-methoxo-μ-alkoxo(bzacbu)-bridged dinuclear units are associated by further bridging of the μ-alkoxo-oxygen atom of $bzacbu^{3-}$ with distances of 2.532(8) Å [Cu2–O3″] and 2.535(7) Å [Cu4–O7′], resulting in different coordination spheres of the copper atoms. The coordination geometries of the Cu1 and Cu3 atoms can be regarded as a planar NO_3 environment because of the long distances of Cu1···N2″ [3.329(12) Å] and Cu3···N4′ [3.334(10) Å], whereas the coordination spheres of the Cu2 and Cu4 atoms have a distorted square-pyramidal NO_4 donor set. From this structural feature, the Cu1–O3–Cu2 [99.6(3)°], Cu1–O4–Cu2 [100.5(3)°], Cu3–O7–Cu4 [101.1(3)°], and Cu3–O8–Cu4 [100.6(4)°] angles may be considered to be important in the magnetic exchange property of **4**.

The crystal structure of **6** is shown in Fig. 13. The molecule has a unique tetranuclear structure, where the four copper atoms are arranged in a tetrahedral array around the central oxo atom (O4), which is located at the crystallographic C_2 axis. The tetrahedron around the oxo atom shows considerable distortion. The bond angles vary from 96.6(10)° for Cu1–O4–Cu2 to 148.0(6)° for Cu2–O4–Cu2′ with Cu–O distances of 1.942(3) and 1.950(5) Å. The Cu1 and Cu2 atoms are bridged by the alkoxo-oxygen atom (O3) of bzacpen and the oxo atom. Each copper atom takes a planar arrangement with the keto-oxygen, amino-nitrogen, and alkoxo-oxygen atoms of bzacpen and the oxo atom. The tetranuclear core found here is different from the previously reported similar tetranuclear copper(II) species in which the central oxygen atom is surrounded tetrahedrally by four octahedral copper atoms.[42] The planar arrangement of each copper atom of **6** may be caused by the steric hindrance of the benzoyl group of the other $bzacpro^{3-}$,

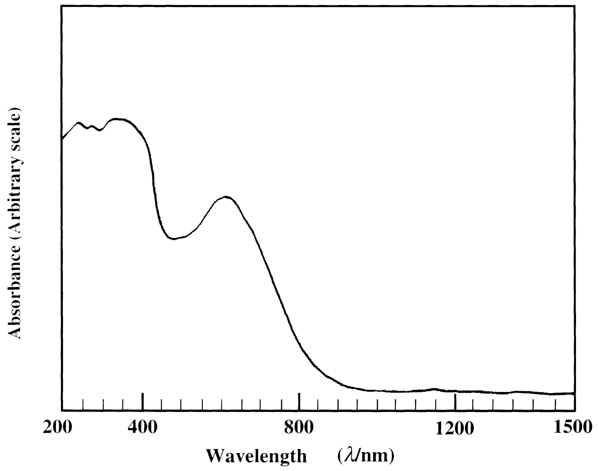

Fig. 14. Diffuse reflectance spectrum of [Cu_2(bzacpro)(CH_3CO_2)] (**1**).

which excludes the axial ligation.

The diffuse reflectance spectra of the present complexes are similar, and are characterized by an intense absorption at near-UV and an absorption band at 570–660 nm. The diffuse reflectance spectrum of **1** is shown in Fig. 14 as a representative example. The shoulder band around 332–404 nm can be assigned as a charge-transfer transition from bridging alkoxo-oxygen to copper(II), although the band is not a distinctive one.[7–9] The absorption spectra in CH_2Cl_2 for the complexes show a d–d transition band at 566–658 nm, depending on the coordination geometries of the copper ions, followed by a charge-transfer transition band at about 350 nm.

The magnetic susceptibilities were measured over the temperature range 4–300 K. The magnetic moments of dinuclear complexes, **1** and **3**, are 2.14 and 2.17 μ_B, respectively, at room temperature, which are lower than the spin-only value, 2.45 μ_B, for two non-interacting $S = 1/2$ copper(II) ions. As shown in Fig. 15, the magnetic moments of both complexes decrease to ca. 0.12 and 0.13 μ_B, respectively, at 4 K. The temperature dependence of the magnetic susceptibilities was analyzed by the Bleaney–Bowers equation based on an isotropic Heisenberg model,[43] $H = -2JS_1 \cdot S_2$,

$$\chi_M = (1-p)\{(2Ng^2\mu_B{}^2/3kT)[1 + (1/3)\exp(-2J/kT)]^{-1}\} + pNg^2\mu_B{}^2/2kT + 2N\alpha, \tag{1}$$

where J is an exchange integral for the two copper atoms and $N\alpha$ represents the temperature-independent paramagnetism, which was set to 60×10^{-6} cm^3 mol^{-1} for each copper atom; the other symbols have their usual meanings. A correction for a small amount (p) of paramagnetic impurity ($S = 1/2$) was taken into account. The best-fitting parameters obtained were $g = 2.01$, $2J = -168$ cm^{-1}, and $p = 0.0061$ for **1** and $g = 2.11$, $2J = -238$ cm^{-1}, and $p = 0.0078$ for **3**. For di-μ-hydroxo-bridged dinuclear copper(II) complexes, a linear relationship was found between the magnetic exchange coupling ($2J$) and the Cu–O–Cu angle.[44] The exchange coupling is antiferromagnetic for Cu–O–Cu angles greater than 97.5°, and an increase of the bridging angle leads to an increase in the antiferromagnetic coupling. A similar correlation exists for alkoxo-bridged dinuclear copper(II) complexes.[1,2] Judging from the fact that the Cu–O–Cu angles are 131.8(3)° for **1** and 125.1(4) and 125.3(3)° for **3**, the magneto-structural correlation would indicate strong antiferromagnetism. However, the observed antiferromagnetic coupling seems to become weak in the present μ-alkoxo-μ-acetato-bridged dinuclear complexes. The $2J$ values are comparable to those ($2J = -95$– -207 cm^{-1}) observed for analogous μ-acetato-μ-alkoxo-bridged dinuclear copper(II) complexes, which show depressed antiferromagnetic coupling due to a "countercomplementary effect" of the acetato-bridge.[22,31] On the other hand, the room-temperature magnetic moments of tetranuclear complexes [**2**, 3.66 μ_B (300 K); **4**, 3.20 μ_B (300 K); **5**, 2.52 μ_B (300 K); **6**, 2.98 μ_B (300 K)] are comparable to, or lower than, the spin-only value (3.46 μ_B) for four non-interacting d^9 ions. The profiles of the temperature dependence of the magnetic moments of complexes **2**, **5**, and **6** show that an antiferromagnetic interaction is mainly operative, as illustrated in Fig. 16. In the case of **4**, the magnetic moment gradually increases to 3.87 μ_B at 4 K with lowering of the temperature, as shown in Fig. 17, suggesting that the magnetic interaction between the metal ions is ferromagnetic. The magnetic-susceptibility data may be analyzed under a first approximation by using a modified Bleaney–Bowers equation with the Weiss temperature (θ) corrected for an interdimer interaction,

$$\chi_M = (1-p)\{[4Ng^2\mu_B{}^2/3k(T-\theta)][1 + (1/3)\exp(-2J/kT)]^{-1}\} + pNg^2\mu_B{}^2/kT + 4N\alpha, \tag{2}$$

in order to compensate for the tetranuclear cores. Fitting of the magnetic data to this modified Bleaney-Bowers equation was performed for complexes, **2**, **4**, and **5**, which have similar step-like-tetranuclear cores. The values for parameters g, J, θ, and p, determined by the fitting procedure, are as follows: $g = 2.12$, $2J = -52$ cm^{-1}, $\theta = 7.6$ K, and $p = 0.022$ for **2**, $g = 1.80$, $2J = 36$ cm^{-1}, $\theta = 0.5$ K, and $p = 0$ for **4**, and $g = 1.74$, $2J = -219$ cm^{-1}, $\theta = -24$ K, and $p = 0.0087$ for **5**. It can be assumed that complexes **2** and **5** are antiferromagnetic in nature and complex **4** is ferromagnetic, although the fitting results contain some unrealistic g values for **4** and **5**, and do not

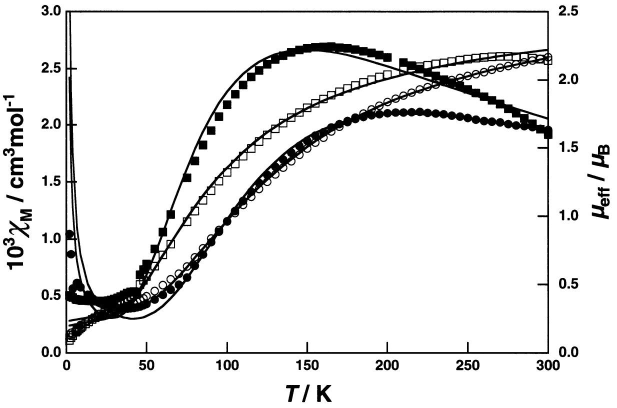

Fig. 15. Magnetic susceptibility data (■, ●) and effective magnetic moments (□, ○) of [Cu_2(bzacpro)(CH_3CO_2)] (**1**)) and [Cu_2(bzacbu)(CH_3CO_2)] (**3**). The solid lines show the best fit obtained (see text).

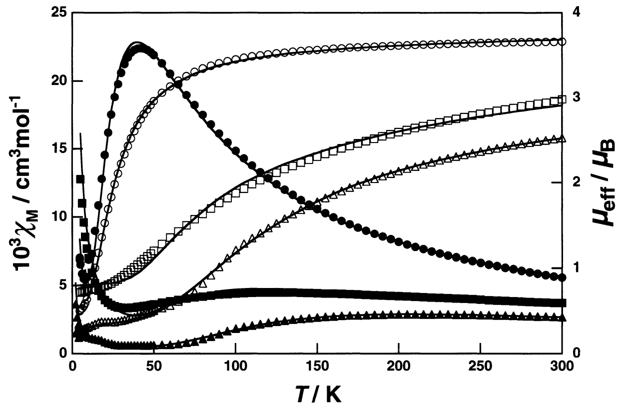

Fig. 16. Magnetic susceptibility data (●, ▲, ■) and effective magnetic moments (○, △, □) of [$Cu_4(bzacpro)_2(C_2H_5O)_2$)] (**2**) [$Cu_4(bzacpen)_2(CH_3CO_2)_2$] (**5**) and [$Cu_4(bzacpen)_2O$]·$H_2O$ (**6**). The solid lines show the best fit obtained (see text).

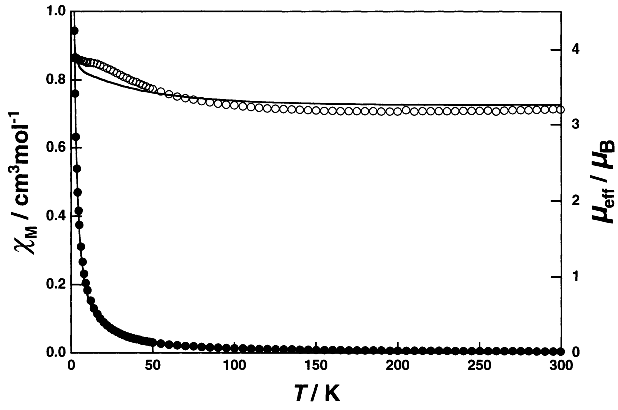

Fig. 17. Magnetic susceptibility data (●) and effective magnetic moment (○) of [$Cu_4(bzacbu)_2(CH_3O)_2$] (**4**). The solid lines show the best fit obtained (see text).

perfectly reproduce the increase in μ_{eff} at low temperature for **4**. Considering the relationship between the 2*J* and the Cu–O–Cu bridging angle, an antiferromagnetic behavior may be expected for **2** and **5**, since most of the important Cu–O–Cu angles are greater than 97.5° [Cu1–O3–Cu2 103.3(2)°, Cu1–O4–Cu2′ 112.7(3)° for **2**, Cu1–O3–Cu2 106.6(1)°, Cu1–O4–Cu2 93.9(1)° for **5**]. On the other hand, the Cu–O–Cu angles of **4** become closer to 97.5° [Cu1–O3–Cu2 99.6(3)°, Cu1–O4–Cu2 100.5(3)°, Cu3–O7–Cu4 101.1(3)°, Cu3–O8–Cu4 100.6(4)° for **4**]. The different magnetic behavior of **4** from the other compounds may be attributed to the small Cu–O–Cu angles. To confirm the ferromagnetic behavior of **4**, the magnetization of **4** versus the applied field was measured (Fig. 18). The magnetization curve of **4** lies above the curve of the Brillouin function for the $S = 1$ state, further supporting the presence of intramolecular ferromagnetic coupling.

In the case of **6**, the data could not be fitted by the modified Bleaney–Bowers equation, and consequently fitted to a more accurate model. The spin Hamiltonian for complex **6**, assuming, an interaction in each pair, can be described in terms of the Heisenberg model,

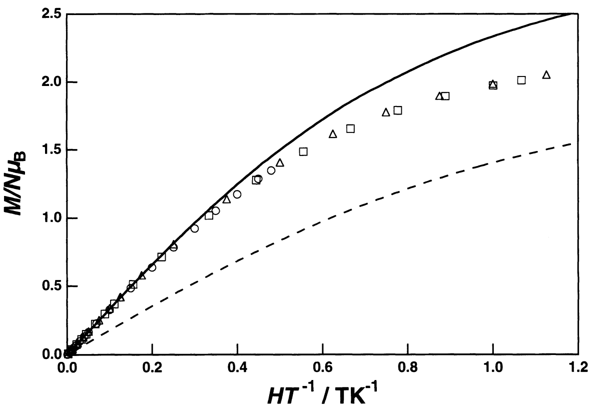

Fig. 18. Field dependence of the magnetization: experimental data for [$Cu_4(bzacbu)_2(CH_3O)_2$] (**4**) at 4 (△), 4.5 (□), and 10 K (○); theoretical curves for $S = 3/2$ (—) and $S = 1$ (- - -) spin states ($g = 2.0$).

$$H = -2[J_1(S_{cu1}\cdot S_{cu2} + S_{cu1'}\cdot S_{cu2'}) + J_2(S_{cu1'}\cdot S_{cu2} + S_{cu1}\cdot S_{cu2'} + S_{cu1}\cdot S_{cu1'} + S_{cu2}\cdot S_{cu2'})], \quad (3)$$

where J_1 refers to the exchange interaction, Cu1–Cu2 and Cu1′–Cu2′, and J_2 to the other copper-copper interactions. The susceptibility can be expressed by Eq. 4, with $x = J_1/kT$ and $y = J_2/kT$.[42]

$$\chi_M = (1 - p)(Ng^2\mu_B{}^2/kT)\{[10\exp(2x) + 2\exp(-2x) + 4\exp(-2y)]/[5\exp(2x) + 3\exp(-2x) + \exp(-4x) + 6\exp(-2y) + \exp(-4y)]\} + p(Ng^2\mu_B{}^2/kT) + 4N\alpha \quad (4)$$

The best-fit parameters were $g = 2.07$, $J_1 = -74$ cm^{-1}, $J_2 = -73$ cm^{-1}, $p = 0.049$ (Fig. 16). The Cu–O–Cu angles concerning to J_1 are 98.9(3)° (Cu1–O3–Cu2) and 96.6(10)° (Cu1–O4–Cu2) for the μ-alkoxo-μ-oxo Cu_2 moieties, whereas the Cu–O–Cu angles concerning to J_2 are 97.4(10)° (Cu1–O4–Cu2′), 127.8(6)° (Cu1–O4–Cu1′), and 148.0(6)° (Cu2–O4–Cu2′) for the mono-μ-oxo Cu_2 moieties. From this feature, it was expected that the J_1 and J_2 interactions could be ferromagnetic and antiferromagnetic, respectively. However, the fitting result does not support this expectation. It is not easy to give a clear explanation of the magnetic properties in terms of the magneto-structural correlation for **6**, although a moderate antiferromagnetic coupling can be expected overall in this system.

Conclusion

Alcoholic-oxygen-containing pentadentate ligands, *N*,*N*′-bis(1-methyl-3-hydroxy-3-phenyl-2-propen-1-ylidene)-1,3-diamino-2-propanol (H_3bzacpro), *N*,*N*′-bis(1-methyl-3-hydroxy-3-phenyl-2-propen-1-ylidene)-1,4-diamino-2-butanol (H_3bzacbu), and *N*,*N*′-bis(1-methyl-3-hydroxy-3-phenyl-2-propen-1-ylidene)-1,5-diamino-3-pentanol (H_3bzacpen) were synthesized and proved to be useful ligands for the synthesis alkoxo-bridged dinuclear and tetranuclear copper(II) complexes which exhibit a diversity of structural types and different magnetic exchange properties as well as oligonuclear complexes of manganese, iron, cobalt, nickel, and zinc ions.

References

1 L. Merz and W. Haase, *J. Chem. Soc. Dalton Trans.*, **1980**, 875.

2 M. Mikuriya, H. Okawa, and S. Kida, *Bull. Chem. Soc. Jpn.*, **55**, 1086 (1982).

3 M. Mikuriya, K. Toriumi, T. Ito, and S. Kida, *Inorg. Chem.*, **24**, 629 (1985).

4 P. de Loth, J.-P. Daudey, H. Astheimer, L. Walz, and W. Haase, *J. Chem. Phys.*, **82**, 5048 (1985).

5 K. Smolander, *Inorg. Chim. Acta*, **128**, 61 (1987).

6 M. Handa, N. Koga, and S. Kida, *Bull. Chem. Soc. Jpn.*, **61**, 3853 (1988).

7 M. Mikuriya, H. Toki, I. Murase, H. Okawa, and S. Kida, *Synth. React. Inorg. Met.-Org. Chem.*, **15**, 965 (1985).

8 M. Mikuriya, *Trends Inorg. Chem.*, **2**, 131 (1991).

9 M. Handa, T. Idehara, K. Nakao, K. Kasuga, M. Mikuriya, N. Matsumoto, M. Kodera, and S. Kida, *Bull. Chem. Soc. Jpn.*, **65**, 3241 (1992).

10 M. Mikuriya, M. Yamamoto, and W. Mori, *Bull. Chem. Soc. Jpn.*, **67**, 1343 (1994).

11 S. Emori, H. Goto, and H. Mitsumasu, *Bull. Chem. Soc. Jpn.*, **69**, 1921 (1996).

12 E. Ruiz, P. Alemany, S. Alvarez, and J. Cano, *J. Am. Chem. Soc.*, **119**, 1297 (1997).

13 K. D. Karlin, *Prog Inorg. Chem.*, **35**, 219 (1987).

14 K. A. Magnus, H. Ton-That, and J. E. Carpenter, *Chem. Rev.*, **94**, 727 (1994).

15 E. I. Solomon, U. M. Sundaram, and T. E. Machonkin, *Chem. Rev.*, **96**, 2563 (1996).

16 a) V. McKee, J. V. Dagdigian, R. Bau, and C. A. Reed, *J. Am. Chem. Soc.*, **103**, 7000 (1981). b) V. McKee, M. Zvagulis, J. V. Dagdigian, M. G. Patch, and C. A. Reed, *J. Am. Chem. Soc*, **106**, 4765 (1984). c) M. G. Patch, H.-K. Choi, D. R. Chapman, R. Bau, V. McKee, and C. A. Reed, *Inorg. Chem.*, **29**, 110 (1990).

17 a) M. Kodera, N. Koura, S. Hosohara, M. Nishimura, M. Ohba, H. Okawa, and S. Kida, *Inorg. Chim. Acta*, **214**, 97 (1993). b) M. Kodera, N. Terasako, T. Kita, Y. Tachi, K. Kano, M. Yamazaki, M. Koikawa, and T. Tokii, *Inorg. Chem.*, **36**, 3861 (1997).

18 R. J. Butcher, G. Diven, G. Erickson, J. Jasinski, G. M. Mockler, R. Y. Pozdniakov, and E. Sinn, *Inorg. Chim. Acta*, **239**, 107 (1995).

19 a) F. Zipped, F. Ahlers, R. Werner, W. Haase, H.-F. Nolting, and B. Krebs, *Inorg. Chem.*, **35**, 3409 (1996). b) P. Gentschev, N. Moller, and B. Krebs, *Inorg. Chim. Acta*, **300-302**, 442 (2000). c) P. Gentschev, M. Luken, N. Moller, A. Rompel, and B. Krebs, *Inorg. Chem. Commun.*, **4**, 753 (2001).

20 a) A. Neves, L. M. Rossi, I. Vencato, V. Drago, W. Haase, and R. Werner, *Inorg. Chim. Acta*, **281**, 111 (1998). b) A. Neves, L. M. Rossi, A. Horn Jr., I. Vencato, A. J. Bortoluzzi, C. Zucco, and A. S. Mangrich, *Inorg. Chem. Commun.*, **2**, 334 (1999).

21 a) W. Mazurek, K. J. Berry, K. S. Murray, M. J. O'Connor, M. R. Snow, and A. G. Wedd, *Inorg. Chem.*, **21**, 3071 (1982). b) W. Mazurek, B. J. Kennedy, K. S. Murray, M. J. O'Connor, J. R. Rodgers, M. R. Snow, A. G. Wedd, and P. R. Zwack, *Inorg. Chem.*, **24**, 3258 (1985). c) W. Mazurek, A. M. Bond, M. J. O'Connor, and A. G. Wedd, *Inorg. Chem.*, **25**, 906 (1986).

22 a) Y. Nishida, M. Takeuchi, K. Takahashi, and S. Kida, *Chem. Lett.*, **1983**, 1815. b) Y. Nishida, M. Takeuchi, K. Takahashi, and S. Kida, *Chem. Lett.*, **1985**, 631. c) Y. Nishida and S. Kida, *J. Chem. Soc., Dalton Trans.*, **1986**, 2633.

23 T. Toki, M. Mikuriya, H. Okawa, I. Murase, and S. Kida, *Bull. Chem. Soc. Jpn.*, **57**, 2098 (1984).

24 W. M. Davis and D. H. Busch, *Acta Crystallogr., Sect C*, **43**, 639 (1987).

25 a) Y. Nishida and S. Kida, *Inorg. Chem.*, **27**, 447 (1988). b) T. N. Doman, D. E. Williams, J. F. Banks, R. M. Buchanan, H.-R. Chang, R. J. Webb, and D. N. Hendrickson, *Inorg. Chem.*, **29**, 1058 (1990).

26 a) J. A. Bonadies, M. L. Kirk, M. S. Lah, D. P. Kessissoglou, W. E. Hatfield, and V. L. Pecoraro, *Inorg. Chem.*, **28**, 2037 (1989). b) J. A. Bonadies, M. J. Maroney, and V. L. Pecoraro, *Inorg. Chem.*, **28**, 2044 (1989). c) K. Bertoncello, G. D. Fallon, K. S. Murray, and E. R. T. Tiekink, *Inorg. Chem.*, **30**, 3562 (1991). d) M. Mikuriya, Y. Yamato, and T. Tokii, *Bull. Chem. Soc. Jpn.*, **65**, 1466 (1992). e) A. Gelasco, M. L. Kirk, J. W. Kampf, and V. L. Pecoraro, *Inorg. Chem.*, **36**, 1829 (1997).

27 a) M. Mikuriya, S. Kida, and I. Murase, *Chem. Lett.*, **1988**, 35. b) Y. Nishida, N. Oshino, and T. Tokii, *Z. Naturforsch., B:* **43**, 472 (1988). c) M. Mikuriya, Y. Yamato, and T. Tokii, *Inorg. Chim. Acta*, **181**, 1 (1991). d) M. Mikuriya, Y. Yamato, and T. Tokii, *Chem. Lett.*, **1991**, 1429. e) M. Mikuriya, Y. Yamato, and T. Tokii, *Bull. Chem. Soc. Jpn.*, **65**, 2624 (1992). f) C. Palopoli, B. Chansou, J.-P.Tuchagues, and Signorella, *Inorg. Chem.*, **39**, 1458 (2000).

28 M. Mikuriya, T. Sasaki, A. Anjiki, S. Ikenoue, and T. Tokii, *Bull. Chem. Soc. Jpn.*, **65**, 334 (1992).

29 a) D. L. Jameson, C. L. Xie, D. N. Hendrickson, J. A. Potenza, and H. J. Schugar, *J. Am. Chem. Soc.*, **109**, 740 (1987). b) Q. Chen, J. B. Lynch, P. G. Romero, A. B. Hussein, G. B. Jameson, C. J. O'Connor, and L. Que, Jr., *Inorg. Chem.*, **27**, 2673 (1988). c) S. Menage, B. A. Brennan, C. J. Garcia, E. Munck, and L. Que, Jr., *J. Am. Chem. Soc.*, **112**, 6423 (1990). d) Y. Hayashi, M. Suzuki, A. Uehara, Y. Mizutani, and T. Kitagawa, *Chem. Lett.*, **1992**, 91. e) Y. Dong, S. Menage, B. A. Brennan, T. E. Elgren, H. G. Jang, L. L. Pearce, and L. Que, Jr., *J. Am. Chem. Soc.*, **113**, 1851 (1993). f) Y. Hayashi, T. Kayatani, H. Sugimoto, M. Suzuki, K. Inomata, A. Uehara, Y. Mizutani, T. Kitagawa, and Y. Maeda, *J. Am. Chem. Soc.*, **117**, 11220 (1995). g) J. H. Satcher, Jr., A. L. Balch, M. M. Olmstead, and M. W. Droege, *Inorg. Chem.*, **35**, 1749 (1996). h) A. L. Freig, M. T. Bautista, and S. J. Lippard, *Inorg. Chem.*, **35**, 6892 (1996). i) M. Suzuki, S. Fujinami, T. Hibino, H. Hori, Y. Maeda, A. Uehara, and M. Suzuki, *Inorg. Chim. Acta*, **283**, 124 (1998). j) H. Sugimoto, T. Nagayama, S. Maruyama, S. Fujinami, Y. Yasuda, M. Suzuki, and A. Uehara, *Bull. Chem. Soc. Jpn.*, **71**, 2267 (1998).

30 S. Wang, S. J. Trepanier, J. C. Zheng, Z. Pang, and M. J. Wagner, *Inorg. Chem.*, **31**, 2118 (1992).

31 T. Kawata, M. Yamanaka, S. Ohba, Y. Nishida, M. Nagamatsu, T. Tokii, M. Kato, and O. W. Steward, *Bull. Chem. Soc. Jpn.*, **65**, 2739 (1992).

32 a) Y. Nakao, M. Yamashita, T. Itoh, W. Mori, S. Suzuki, and T. Sakurai, *Bull. Chem. Soc. Jpn.*, **67**, 260 (1994). b) C. Li, N. Kanechisa, Y. Miyagi, Y. Nakao, S. Takamizawa, W. Mori, and Y. Kai, *Bull. Chem. Soc. Jpn.*, **70**, 2429 (1997).

33 T. Kayatani, Y. Hayashi, M. Suzuki, K. Inomata, and A. Uehara, *Bull. Chem. Soc. Jpn.*, **69**, 389 (1996).

34 J. H. Satcher, M. W. Droege, T. J. R. Weakley, and R. T. Taylor, *Inorg. Chem.*, **34**, 3317 (1995).

35 W. F. Zeng, C. P. Cheng, S. M. Wang, and G.-H. Lee, *Inorg. Chem.*, **35**, 2259 (1996).

36 a) M. Mikuriya, K. Majima, and Y. Yamato, *Chem. Lett.*,

1992, 1929. b) M. Mikuriya, N. Nagao, and K. Kondo, *Chem. Lett.*, **2000**, 516. c) M. Mikuriya and K. Minowa, *Inorg. Chem. Commun.*, **3**, 227 (2000). d) M. Mikuriya, K. Minowa, and J.-W. Lim, *Bull. Chem. Soc. Jpn.*, **74**, 331 (2001). e) M. Mikuriya, K. Minowa, and N. Nagao, *Bull. Chem. Soc. Jpn.*, **74**, 871 (2001). f) M. Mikuriya, K. Minowa, and N. Nagao, *Inorg. Chem. Commun.*, **4**, 441 (2001).

37 P. W. Selwood, "Magnetochemistry," Interscience Publishers, New York (1956), pp. 78, 91.

38 C. K. Fair, "MolEN Structure Determination System," Delft Instruments, Delft, The Netherlands (1990).

39 K. Nakamoto, "Infrared and Raman Spectra of Inorganic and Coordination Compounds," 4th ed, Wiley interscience, New York (1986).

40 M. Mikuriya, S. Kida, and I. Murase, *Bull. Chem. Soc. Jpn.*, **60**, 1681 (1987).

41 R. L. Rardin, W. B. Tolman, and S. J. Lippard, *New. J. Chem.*, **16**, 417 (1991).

42 a) S. Teipel, K. Griesar, W. Haase, and B. Krebs, *Inorg. Chem.*, **33**, 456 (1994). b) J. Reim, K. Griesar, W. Haase, and B. Krebs, *J. Chem. Soc., Dalton Trans.*, **1995**, 2649.

43 B. Bleaney and K. D. Bowers, *Proc. R. Soc. London, A*, **214**, 451 (1952).

44 a) D. J. Hodgson, *Prog. Inorg. Chem.*, **19**, 173 (1975). b) W. E. Hatfield, "Theory and Applications of Molecular Paramagnetism," ed by E. A. Boudreaux and L. N. Mulay, Wiley-Intersciecne, New York (1976).